Autonomous battery less sensor for IoT applications in Smart Buildings

Low-power Energy Conversion and Storage for RF Energy Harvesting

by

D. A. Bosma & W. P. Lindeman

to obtain the degree of Bachelor of Science
at the Delft University of Technology.

Project duration:	April 23, 2018 – July 6, 2018	
Thesis committee:	dr.ir. G. (Ger) de Graaf	Supervisor
	prof. dr. ir. S. (Said) Hamdioui,	Chairman jury
	dr. ing. I. (Ioan) Lager	Jury member
Proposer:	prof. dr. ir J. E. J. (John) Schmitz	Jury member

TU Delft

Preface

This report discusses one part of a project consisting of three parts. The goal of the project is to design a battery less sensor powered by RF energy fields present in an office environment. The sensor is able to measure the temperature and is able to communicate wirelessly using a low power communication protocol. In this project the use case of a building will be explored, where the climate and lighting of different rooms can be adapted, be monitored and be adjusted remotely. Commissioned by the dean of faculty EEMCS of the University of Technology Delft dr. John Schmitz this project has started as a Bachelor Graduation Project for the BSc. Electrical Engineering. This project was assigned to a group consisting of two students per subgroup, six students in total.

In this report the energy conversion and storage of the system will be discussed. A high-frequency signal coming from an antenna must be converted to an output signal which is functional for the communication module. Therefore a steady 3.3 V DC output needed to be created with a rectifier circuit. In order to achieve maximum power transfer to the load, a matching circuit with the RF energy harvesting antenna needed to be designed. The main challenges were to achieve a high enough input voltage to reach the threshold voltage of the diodes of the rectifier and to rectify the AC input as efficient as possible. To tackle these challenges a design with a Greinacher rectifier with low-threshold Schottky diodes and a DC/DC booster is presented. In Fig. 1 a picture of the final design can be seen.

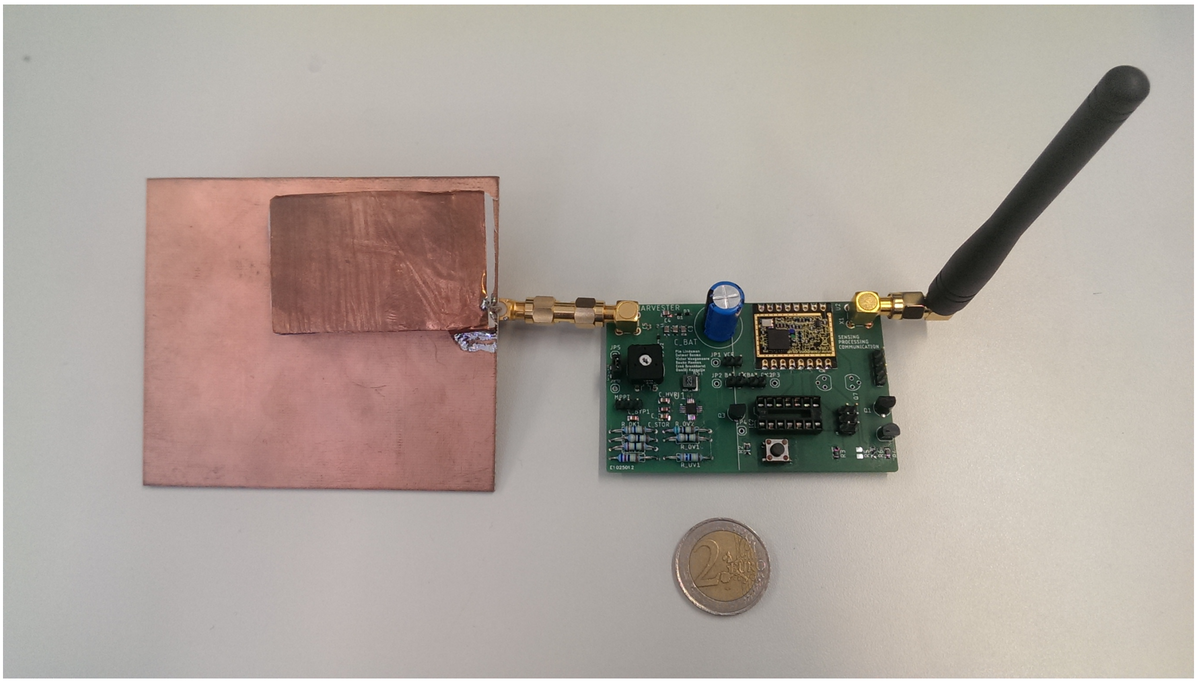

Figure 1: Final design

Contents

List of Figures

1
Introduction

All electronics devices need a power source. For most small electronics this tends to be some form of battery. This battery can be recharged with a battery charger or can be replaced by another battery. However nowadays more and more electronic devices can be charged wirelessly by using inductive coupling, capacitive coupling or magnetodynamic coupling. Applications of these techniques are charging mobile phones, electrical toothbrushes, biomedical microsystems [1] and even electrical driven cars can be charged wirelessly [2].

These charging techniques are based on the experiments of inventor Nikola Tesla. He experimented with lighting a lamp by using of resonant inductive coupling of two LC-circuits, varying the physical distance between the transmitter and the receiver. These experiments of Tesla have still impact on today's technology, like he wanted in his days:

> "As regards the production of light, some results already reached are encouraging and make me confident in asserting that the practical solution of the problem lies in the direction I have endeavored to indicate. Still, whatever may be the immediate outcome of these experiments I am hopeful that they will only prove a step in further developments towards the ideal and final perfection." - Nikola Tesla [3]

All these applications are dependent on an external energy source, but what if a device does not need a battery and can operate autonomously? One of the solutions is Radio-Frequency (RF) energy harvesting. An energy conversion technique where electromagnetic waves on ultra high frequencies (UHF), which are present almost everywhere, are transformed into electric power. Billions of radio transmitters everywhere in the world are broadcasting RF energy, including mobile telephones, mobile base stations (GSM), television broadcast stations, radio broadcast stations and internet modules (WiFi/3G/4G). This RF energy can be harvested from ambient sources and can be used for wireless charging. With this technique a very low energy consuming device, like a temperature sensor, can operate without using a battery and can be placed anywhere.

1.1. Problem definition

RF-energy harvesting is a present-day technique which was not a common alternative for energy harvesting in the past. The reason for this was the availability of RF energy. A couple of decades ago very little RF energy was available compared to now, due to the fact that today mobile phones are used more and more and internet becomes more important. Electronics are also becoming more and more power efficient, making RF harvesting more viable. At this moment some companies are experimenting with autonomous sensors, like NOWI-energy [4], Freevolt [5] and Powercast [6]. These products make use of RF energy harvesting to extend the lifetime of the battery of the device. The goal of RF energy harvesting techniques is to have a device that does not need a battery and consumes only energy from electromagnetic waves on radio frequencies. This is very useful for all Internet-Of-Things (IoT) applications. Millions of sensors will be used for this technology, and one can imagine that it is not feasible to change the batteries of all these sensors every now and then or to pull cables everywhere to connect the sensors to the grid.

Therefore a solution will be presented. In this project a device will be designed that will power a temperature sensor with RF energy harvesting and communicate the data wirelessly to a base station, *without using a battery*. This base station will upload the data to "the cloud", where the data will be stored. This feature is necessary for the IoT-applications. An overview of the system can be seen on Fig. 1.1. To harvest the RF energy an antenna will be used and will be matched to a rectifier, which converts the ultra high frequency signal to DC. The energy will be stored in a capacitor and will be used to power the temperature sensor and the data processing unit, which collects the data and transmits it to a base station. With this system design no battery will be needed. The goal is to harvest as much energy as available and to use this energy as efficiently as possible.

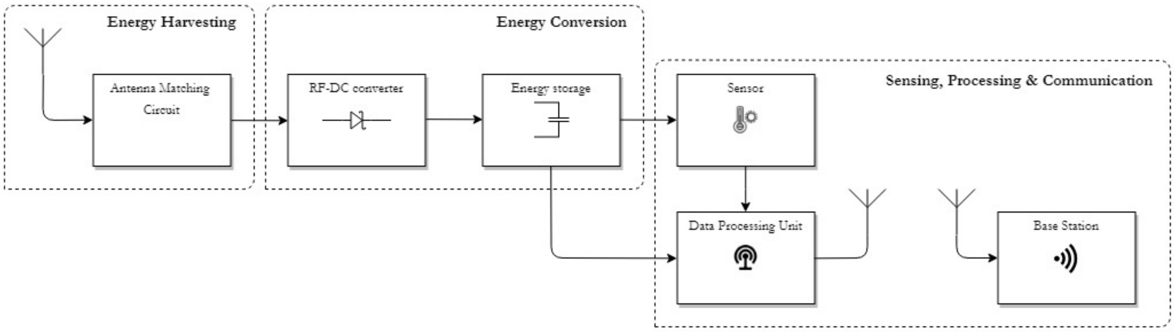

Figure 1.1: System overview

This device can be placed everywhere and will operate for a theoretically infinite amount of time, without the need for occasional battery replacements and without using cables to provide the device with energy from an external energy source. With this device it is very easy to measure environmental parameters at every location if enough RF energy is available. By collecting all the data in "the cloud", these devices can be used in Smart Buildings: building automation for energy consumption [7]. A category of control and communications technologies that link building systems that are typically controlled separately. This can be systems for electrical distribution, fire alarming, security, heating and air conditioning [8]. The design will succeed if a single sensor is produced that can be powered by ambient RF energy harvesting, without the use of a battery.

It is possible to design a system with these features, but the system is dependent on the available RF energy at the location where the device is placed. The level of ambient RF energy affects the frequency at which the system can harvest and communicate. A reduction in RF energy means that the period between each time the data can be communicated increases. Additionally a minimum level of available energy has to be reached to convert the RF energy to a voltage level that can be used by the system. To achieve the best performance each of the subsystems have to be optimized and matched to each other. The performance of the whole system is best observed by looking at the sense-and-communicate interval.

2

Programme of Requirements

2.1. Requirements of whole system

The goal of this project is to build an *Autonomous battery less sensor for IoT-applications in Smart Buildings*. This chapter will present the requirements of the whole system and the special requirements for the subsystem discussed in this report.

2.1.1. Technical specifications

1-1 Cloud
The sensor should be an IoT-device, which means that it is connected to the cloud. This can be concretized as follows: the device must communicate its measured values to another device (base station or service) which on its turn will make the information available over internet. In other words, the device does not have to be directly connected to the internet per se, as long as its information becomes available on the internet.

1-2 Smart building
The device is intended for use in so called *Smart Buildings*. A Smart Building in this sense uses many sensors and actuators to control for example the climate (temperature, humidity, air quality) or security autonomously, so without the intervention of a human person [7].

1-3 Self powered
There should be no need to physically access the device on a regular basis. This means the device cannot use batteries, because they need replacement every now and then. Also, in order to be versatile and easy to place anywhere, the device should not use a wired power source. The device should therefore be able to extract energy from its environment and this should be done by the use of RF harvesting.

1-4 Measured quantity
For this project, it is sufficient to just measure ambient temperature. This should be possible with a precision of about 0.1 °C. Furthermore, the device must be designed in such a way that at a later stage, the temperature sensor could easily be replace with a different sensor (e.g. humidity or light intensity).

1-5 Integrity
The device should ultimately be used in a Smart Building, thus be connected to certain actuators in an autonomous fashion. It is therefore essential that the data produced by the device is correct. There must be a form of error checking, so that faulty data is discarded.

1-6 Redundancy
The device completely depends on ambient RF sources and in case these are non-existent or the power that can be extracted from them is too little, the device will be unable to function. This is acceptable and should be considered in the application of the IoT-sensors, they might not function from time to time due to lower levels of RF energy. Having many sensors in different locations obviously reduces the chance that no sensor in a certain vicinity functions, so this is a way to overcome the problem.

1-7 Production cost
The devices should be used on large scale, i.e. many sensors should be placed in a building. This requires that the production cost of a single sensor is limited and should not exceed €50.

1-8 Configuration
Either the device must be designed in such a way that no configuration is needed, i.e. it can just be placed somewhere and work right away. Otherwise, the device must have an interface so a serviceman can configure the necessary settings on site.

1-9 Security
The data coming from the device must be secured, so that it is not possible for anyone to interfere. It should not be possible to mimic the device, nor should the data be readable by anything other than the intended receiver.

2.1.2. Geometric specifications

2-1 Office Environment
The IoT-sensor will be designed for operation in an office environment. This office environment is considered to be on the mainland, i.e. to be covered by the GSM-network and not to be exposed to abnormal amounts of RF (e.g. near a microwave oven).

2-2 Location
The IoT-sensor will be designed for operation in the EU. Transmission of RF fields is regulated by the EU defined rules for RF transmission. Also the harvesting of RF is based on operating frequencies in the EU.

2-3 Dimensions
Since the IoT-sensor is designed for use in an office environment, the actual size of the sensor is of great importance. The sensor should not interfere with the architectural and constructive aspects of the Smart Building. The maximum size of the sensor should be somewhat equal to that of a normal enterprise grade WiFi access-point. The maximum dimensions are therefore defined as 200x200x100 mm (LxWxH).

2.1.3. Environmental specifications

3-1 Water & dust resistance
The IoT-sensor is designed for indoor use only. Since office environments are known to be not extremely dusty only a case to protect the hardware to big objects is necessary. Therefore the case will comply to IP1X dust protection (protection against objects bigger than 50mm). And since the sensor is designed for indoor use only, it will comply to IPX0 water protection (no special protection) [9].

3-2 Operating temperature
Since the IoT sensor is designed for indoor use only, the operating temperature will be 0-40°C. Assuming that an office will always be above 0°C because it is indoors. The maximum temperature of +40°C gives the capability to measure in (relative) hot rooms, like server rooms.

3-3 Overvoltage & Brown-out
As the input power (RF power) fluctuates quite randomly over time, there might be moments where there is a lot of power available and moments where there is very little. The device must be protected for sudden high levels of power, so that the device is not damaged. Also, the device must be able to cope with very little amounts of power, as this could corrupt the data registers if no care is taken.

3-4 Orientation
Since the antenna for the RF harvesting, implemented on the IoT sensor, is direction-sensitive, the direction of installation will be important. The direction of installation will be defined by the antenna design, and therefore determined at installation.

3-5 Minimal available RF power
In order to be able to harvest energy from the RF waves available in the office environment, the amount of available power has to be at least -25 dBm. This value is based on background radiation, measured by a vector network analyzer.

2.2. Requirements of subsystem

Since the conversion module is the bridge between the antenna and the communications module most of the requirements are defined by these two subsystems. The antenna defines the operating frequency, the maximum and average available power and the input impedance [10]. The communications module defines the output voltage and energy storage requirements. The communications module also requires that no power is being delivered to the load when not enough energy is stored to make a measurement [10]. The performance of the whole system is dependent on the sense-and-communicate interval. This interval has to be as small as possible but it is really dependent on its environment and the available ambient RF-energy. Therefore it is not a requirement, but something to keep in mind while designing the subsystem. The requirements of the subsystem are:

4-1 The subsystem must convert the input voltage to a DC output voltage.

4-2 The subsystem must have a DC output voltage higher then 2.7 V, since this is the required minimum voltage of the micro controller of the communication module.

4-3 The subsystem must have a DC output voltage lower then 3.9 V, since this is the required maximum voltage of the micro controller of the communication module.

4-4 The subsystem must be able to convert the input voltage with a power peak equal to -25 dBm.

4-5 The subsystem must store all energy until an energy level of 4 mJ is reached, since this is the amount of energy needed to transmit one sensor measurement data package.

4-6 The subsystem must send a signal to the communication module if enough energy is harvested to send a data measurement.

4-7 The subsystem should have a nominal DC output voltage equal to 3.3 V, since this is the required input voltage of the sensor.

4-8 The subsystem should have an input impedance equal to the impedance of the antenna in order to have maximum power transfer.

4-9 The subsystem should be able to operate with input frequencies from 800 MHz up to 900 MHz, since this frequency band will be used by the antenna module.

The voltage specifications are based on the chips used in the communications part. They are simply the voltages at which these chips can safely and reliably operate. The storage requirements are based on the energy required to do a single measurement and send the result to a central server. More details on this can be found in [10].

The specifications for the power received and working frequency are obtained using a spectrum analyzer. More details on how this is done can be found in [11]. Most antennas have a 50 Ω input impedance, as this is the industry standard. Because the conversion and harvesting module where developed in parallel the decision was made to match both of these systems to 50 Ω. In the final design both matching circuits have been combined for improved efficiency.

3
Design

In this section the design of the subsystem for energy conversion and storage will be discussed. The design is divided into three parts: rectification, conversion and storage.

3.1. Rectification

The input of the conversion unit is the RF-signal coming directly from the antenna. In order to store the power from this signal it needs to be converted to DC. For this a rectifier circuit is required. The specifications of the rectifier circuit can be found in Tab. 3.1. The specifications for the output voltage are based on the DC/DC-converter which is attached to the output of the rectifier. More information on this can be found in section 3.2. The other specifications are based on the requirements found in chapter 2.

Table 3.1: Rectifier specifications

Parameter	**Value**
$V_{\text{out, min}}$	80 mV
$V_{\text{out, peak}}$	330 mV
f_{input}	800-900 MHz
$P_{\text{in, peak}}$	-25 dBm

Because the expected signal power is very low, the voltage of the incoming signal will also be very low. This low input voltage is problematic when using a conventional full-bridge rectifier (see Fig. 3.1), since the voltage lost over the diodes is too great compared to the output voltage (see eq. 3.1). Most low power rectifiers use either a Dickson (section 3.1.2) or a Greinacher (section 3.1.3) configuration, which are less effected by the diode threshold voltage and are therefore more suitable for low-voltage rectification. Both these configurations can be expanded by adding multiple stages to the rectifier (see Appendix A), stepping up the voltage even further [12][13]. In order to minimize the effects of the diode threshold further most rectifiers designs used in RF harvesting use either low threshold voltage Schottky diodes (section 3.1.1) or some form of V_{th}-cancelling transistor configuration with CMOS-transistors [14]. In this project Schottky diodes are used, as designing and producing an IC was deemed unfeasible and would likely only provide a marginal performance improvement at best.

$$V_{full-bridge} = \frac{1}{2} V_{pp} - V_{th} \tag{3.1}$$

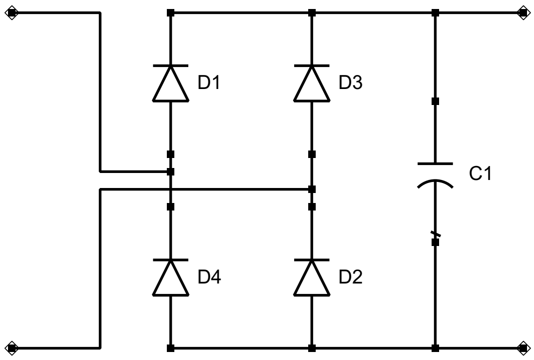

Figure 3.1: Schematic of a full-bridge rectifier.

3.1.1. Schottky diode

The goal of the design is to convert the available ambient RF energy as efficient as possible on a certain frequency. To improve the efficiency of the rectifier the diode threshold and capacitance has to be as low as possible and the leaking current as little as possible. Therefore a Schottky diode is the most appropriate type of diode. A Schottky diode is a special type of diode built on a metal-semiconductor substrate and has a very low threshold voltage (typically 0.15 V - 0.4 V) and a junction capacitance of about 18 pF [15][16]. The disadvantage of a Schottky diode is the high manufactering costs. In Fig. 3.2 and Fig. 3.3 the DC- and AC-characteristics of three Schottky diodes typically used in RF harvesting circuits can be seen [17][18]. Simulations have been done with Advanced Design System (ADS) and the frequency used for the AC-simulation was set on 845 MHz, as most power is available at this frequency [11]. The SMS7630 is used in the final design, as it had the lowest threshold voltage, fastest switching time and least amount of leakage.

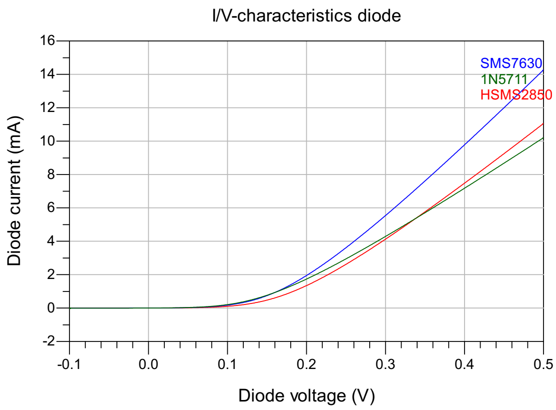

Figure 3.2: DC-characteristics of Schottky diodes

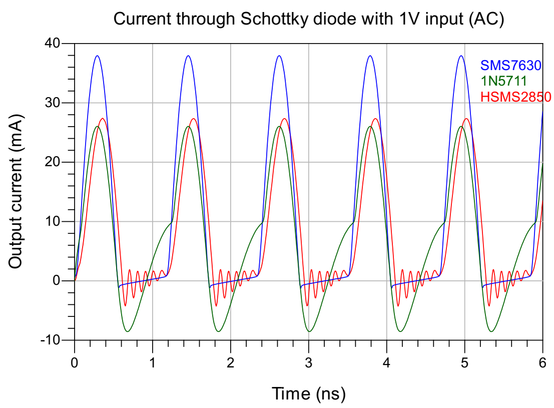

Figure 3.3: AC-characteristics of Schottky diodes

3.1.2. Dickson rectifier

A very common rectifier design used in energy harvesting is the Dickson rectifier [13][19]. A Dickson rectifier works on the basis of a charge pump (see Fig. 3.4). During the positive half-period of the sinusoidal voltage applied across diode D1, capacitor C1 will be charged by the current flowing through diode D1. Capacitor C1 is not able to discharge via diode D1, so all current will flow through diode D2 to the load. During the negative half-period the current can flow through diode D1, through diode D2 to the output. Diode D2 also prevents current from the load flowing back into the rectifier. Capacitor C2 operates as storage load and is not a necessary component. A Dickson rectifier is asymmetrical: when the input is negative the current has to pass though two diodes before entering the load, as opposed to a single diode when the input is positive. This means that the Dickson rectifier supplies more power to the load during the positive half of the cycle. The output voltage over capacitor C2 can be calculated with eq. 3.2.

$$V_{Dickson} = V_{pp} - V_{th} \tag{3.2}$$

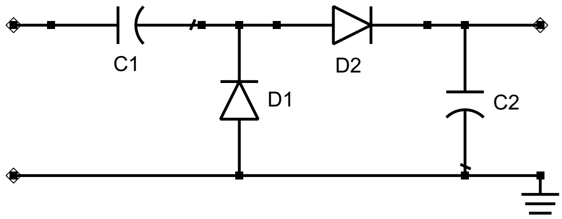

Figure 3.4: Schematic of a Dickson rectifier.

3.1.3. Greinacher rectifier

The Greinacher rectifier aims to solve the asymmetry problem of the Dickson rectifier. It consists of two Dickson rectifiers: one for the positive half-cycle and one for the negative. The output voltages are put in series, resulting in double the output voltage. Its symmetry is also helpful when determining the input impedance, as the input impedance - while still non-linear - is now at least the same for both halves of a cycle. This will be further discussed in section 3.1.4. Because of the higher efficiency and the (slightly) more predictable input impedance the Greinacher rectifier has been adopted in the final design [20]. A multistage rectifier has two configurations: one with all capacitors parallel and one with all capacitors in series. These configurations generally behave the same, but do have some differences in charging speed of the output capacitors [21]. These differences can be seen in Appendix A. The amount of stages that are used is further discussed in section 3.1.4.

$$V_{Greinacher} = 2V_{pp} - 2V_{th} \tag{3.3}$$

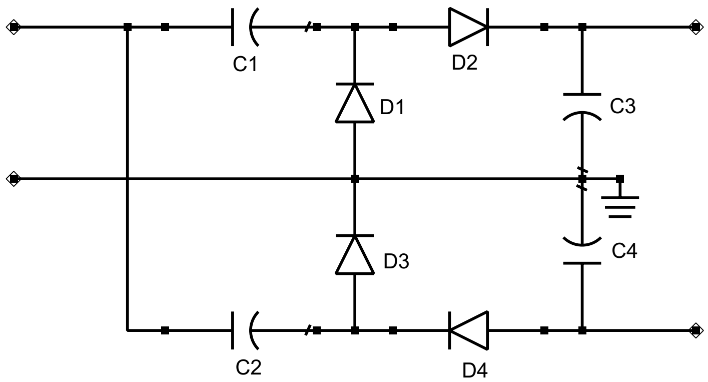

Figure 3.5: Schematic of a Greinacher rectifier.

In order to choose the value of the capacitors in the rectifier, a consideration has to be made between the amount of losses of the capacitor and the functionality of the rectifier. These capacitors are only there to filter DC signals. A larger capacitance results in less losses, but a longer start-up time. In order to determine a proper capacitance value, the magnitude of the impedance of the capacitor has been set at Z_{cap} = 1 Ω. With eq. 3.4 the capacitance can be calculated assuming a frequency equal to 845 MHz, where ω is 2πf. This results in a capacitor of C_i = 188 pF with i=1:4.

$$C = \frac{1}{|Z_{cap}|\omega} \tag{3.4}$$

3.1.4. Input impedance

In order to achieve maximum power transfer to the load, the input impedance of the rectifier should match the impedance of the antenna. Because the antenna subsystem and the converter subsystem were designed in parallel, the impedance of the antenna was unknown. In order to have a properly matched system, the values of the matching components are determined in the end of the design. For now the method of determining the matching circuit is shown, assuming an antenna impedance Z_{ant} = 50*j0 Ω, because this is a standard impedance used in antenna design. If the load impedance is equal to the complex conjugated input impedance, the power transfer is optimal (see Fig. 3.6). To achieve this a matching circuit is needed. In order to design the matching circuit the input impedance of the rectifier needs to be determined accurately [22]. Besides that, the efficiency of the rectifier is dependent on the input voltage and to calculate the input voltage the magnitude of the input impedance must be known.

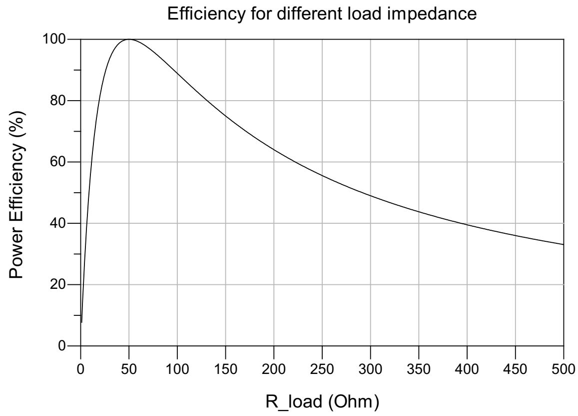

Figure 3.6: Efficiency of power transfer to the load for a 50 Ω source impedance.

Due to the inherent non-linearity of rectifier circuits it is not possible to determine a single input impedance that is valid for the entire duration of a single wave. Because of this the input impedance has been defined as the impedance that would result in the same power being dissipated as the rectifier circuit for one period, as is recommended in [23]. The non-linearity also means that the input impedance is not only frequency dependent but also input power dependent.The non-linearity of the diodes makes it very difficult to model the characteristics of the rectifier. Attempts where made to model the circuit using methods explained in [23]. However, the data sheet of the selected Schottky diode did not provide detailed enough information about the voltage-current and voltage-capacitance characteristics to accurately determine the input impedance. It was therefore decided to simulate the rectifier in ADS. In ADS a simple full wave Greinacher rectifier (see Fig. 3.5 on page 9) is simulated, where the input power P_{in} has been set on -25 dBm. A frequency sweep between 500 MHz and 1200 MHz was done, the results can be seen in figure 3.7 in a Smith Chart. When sweeping the frequency, the input impedance varies very little. This is a good thing, as it allows the circuit to be matched over a wide frequency band. The impedance of the rectifier at -25 dBm and 845 MHz is equal to Z_{in}=Z_0*(1.64-j6.27) Ω, where Z_0 is equal to 50 Ω. In Fig. 3.8 can be seen how the input impedance changes if the input power P_{in} is swept.

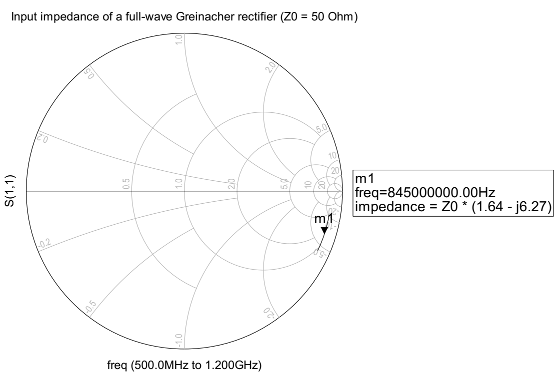

Figure 3.7: Input impedance $|Z_{in}|$ for a single stage rectifier on Smith Chart

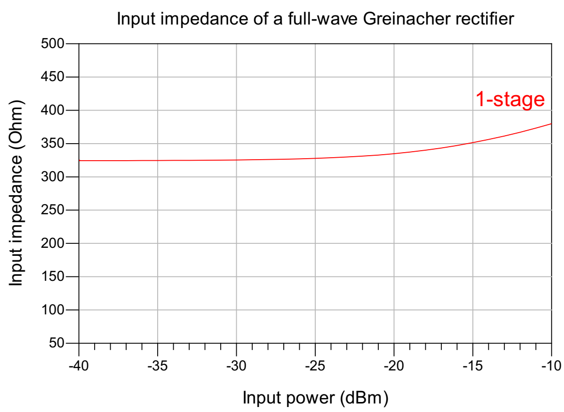

Figure 3.8: Input impedance $|Z_{in}|$ for a single stage rectifier as function of input power

3.1.5. Voltage booster

In order to improve the efficiency of the rectifier the input voltage needs to be as high as possible. This mitigates the losses caused be the diode threshold voltage. Ideally the input impedance of the rectifier is as high as possible as this results in a higher voltage at the input, as can be seen in eq. 3.5, where the factor $\sqrt{2}$ is needed in order to have the voltage amplitude instead of the RMS-voltage. The simulation of this equation can be seen in Fig. 3.9, where the input power P_{in} is fixed on -25 dBm and where `R_load` is equal to R_{in}. While using more stages results in a higher output voltage at the same input voltage, the impedance of a single stage rectifier is significantly higher then that of a multistage one [24], as can be seen in Fig. 3.10. The relative high impedance of a single stage rectifier means that even at lower input power the input voltage is closer to the threshold of the diodes. Overcoming the threshold voltage is crucial to the operation of the rectifier, so a lower amount of stages results in a higher efficiency at lower input power [25], despite of the fact that more stages gives a higher output voltage [26]. Because of this it has been decided to use a single stage rectifier.

$$V_{in} = \sqrt{2P_{in}R_{in}} \tag{3.5}$$

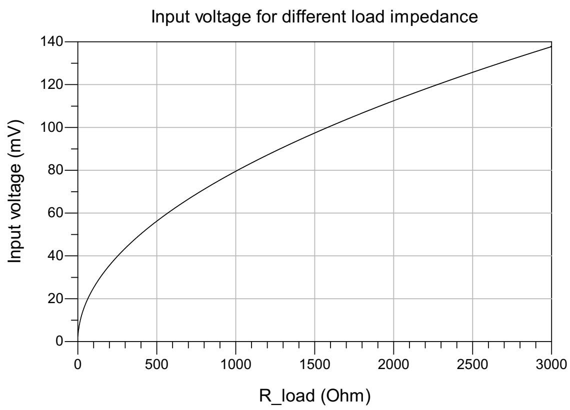

Figure 3.9: Input voltage for different loads.

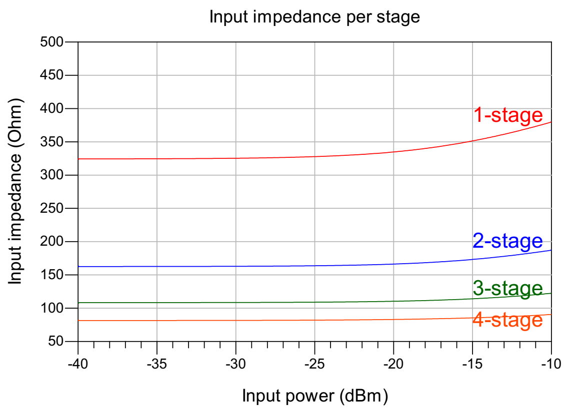

Figure 3.10: Input impedance for different stages

Attempts have been made to artificially increase the input impedance. One method suggested by [27] is to use a resonator, as can be seen in Fig. 3.11. The idea is to use what is essentially a very poorly designed high-pass filter with a very high resonating peak to bump up the voltage at the desired frequency. While this sounds great in theory this idea is fundamentally flawed. The reason a resonator is able to produce such a high voltage is because its impedance is very high at its resonating frequency which, as previously mentioned, results in a higher voltage. All a resonator will end up doing is decrease the bandwidth, increase complexity and increase losses.

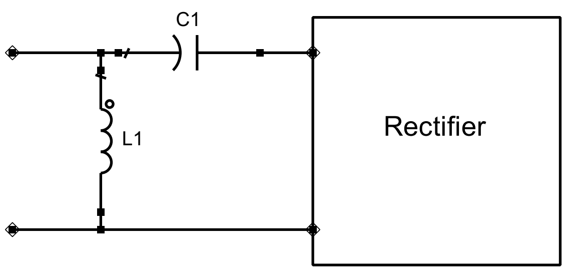

Figure 3.11: Schematic of a resonator.

The only real way of changing the input impedance is by varying the output impedance of the rectifier. This has however proven to be very difficult to simulate. Luckily the output of the rectifier is attached to the DC/DC- converter, which allows its input impedance to be varied with a potentiometer so it can be optimized after production. More on this can be seen in section 3.2.

3.1.6. Impedance matching

The input impedance of the rectifier has a real and an imaginary part and the antenna impedance only consists of a real part. Components with only a pure imaginary impedance, like capacitors and inductors, are placed in series with the rectifier to cancel the reactance of the input impedance. Parallel placed components can be used to alter both the real and imaginary part of the impedance. With the combination of components in series and parallel it is possible to design a perfect matched circuit. With a properly designed matching circuit, the reflection coefficient Γ will be zero and the maximum power transfer will be achieved.

Knowing the input impedance, the rectifier needs to be matched to 50 Ω. Firstly this impedance can be made real by putting an inductor in parallel to it. This is where the large imaginary part of the impedance is very helpful. By putting a 63.8 nH inductor in parallel to the rectifier the total impedance becomes 1439 + 0j Ω at 845 MHz. This is due to the resonating action described earlier, however instead of trying to resonate with an external capacitor the resonation is occurring between the inductor and the rectifier itself [12]. This is the input impedance that should be considered when calculating the voltage at the input of the rectifier.

However the rectifier should not just be made real, but should be matched to the 50 Ω of the antenna. Any impedance can in principle be matched to any other impedance using just a capacitor and an inductor [21], and this is no exception (see Fig. 3.12). Using a Smith Chart a matching circuit with a 27.5 nH inductor in parallel and a 0.754 pF capacitor in series is determined. In Appendix B the Smith Chart is presented. These matching components match the input impedance of the rectifier perfectly to 50 Ω, which can be seen in Fig. 3.13. Because inductors and capacitors are reactive elements no losses should occur, however in practice this is not the case. These losses are sadly unavoidable. In Fig. 3.14 and 3.15 the effects of adding a matching circuit can be found.

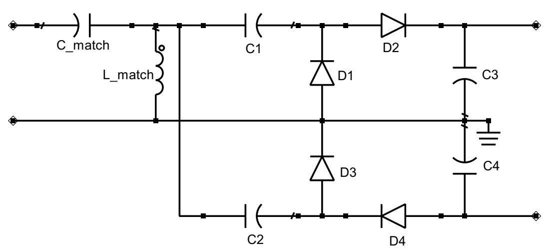

Figure 3.12: Greinacher rectifier with matching circuit

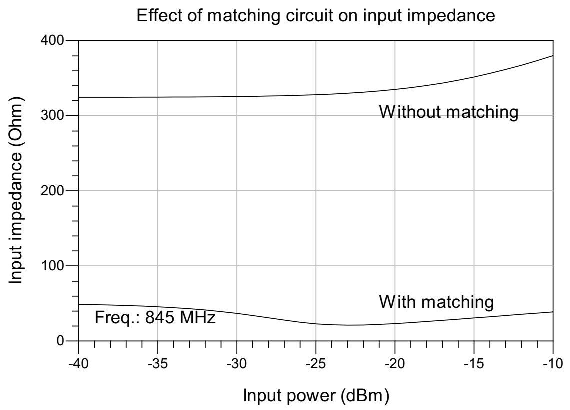

Figure 3.13: Effect of matching circuit on input impedance

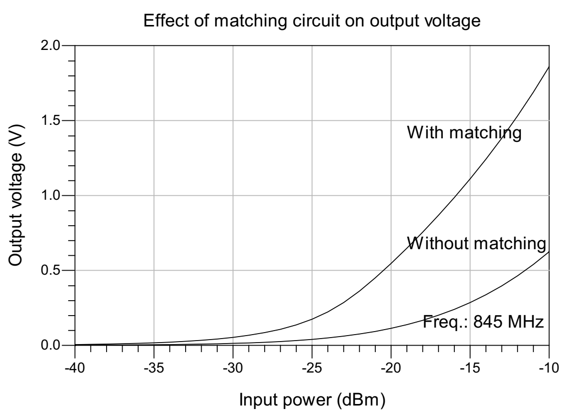

Figure 3.14: Effect of matching circuit on output voltage as a function of input power

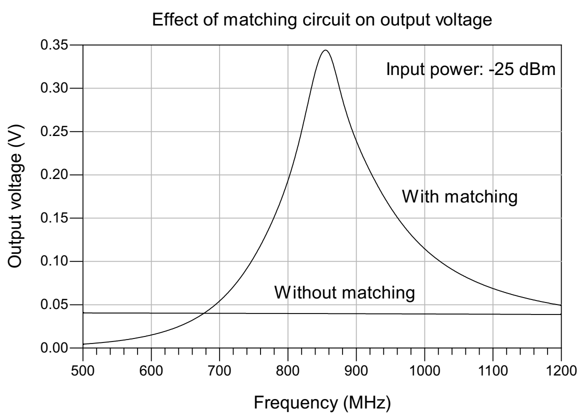

Figure 3.15: Effect of matching circuit on output voltage as a function of frequency

3.2. DC/DC-converter

The output voltage of the rectifier is still too low to operate any type of meaningful electronics, even at the peak input of -25 dBm. It still needs to be booster further in order to be useful in any way. This is done using an off-the-shelf DC/DC-converter. The chosen DC/DC-converter is a BW25504 Ultra Low-Power Boost Converter, as recommended in [18] and [28]. This converter is specially designed for low-power energy harvesting systems. During start-up it requires 330 mV DC at the input. Once the storage device has been charged to 1.5V the device enters normal operation and only requires 80 mV DC at the input to generate 3.3 V at the output [29]. This is significantly better then most DC/DC-converters, as these tend to only start converting at 700 mV or higher at the input.

The start-up input voltage (330 mV) is also the value that is used to set the requirement for the peak output voltage. If for whatever reason the storage voltage drops below 1.5 V, the device should be able to recover. During normal operation however the output voltage should not drop below 1.5 V to allow harvesting even when much lower power is available. After starting up only 80 mV is needed to convert the input voltage to an appropriate output voltage.

This DC/DC-converter is also able to test the storage device for SOC (State Of Charge). The converter outputs a digital `BAT-OK` signal that is dependent on the storage voltage level. This signal is high when enough energy is available to allow for transmission. Once the output voltage drops below a certain level the `BAT-OK` signal goes low. This shuts down power to the communications unit. Because of the reduced load the storage device will be able to charge again. Once the output voltage rises above a second threshold the signal will go high again, allowing another transmission to be made. The thresholds are set using a single 3-stage resistor voltage divider. The total value of the divider is 10 MΩ, as is recommended in the data sheet. In order to have the `BAT-OK` signal turn on at 2.8 V and turn off at 3.7 V a resistor divider with R_1 = 3.24 MΩ, R_2 = 4.32 MΩ and R_3 = 2.43 MΩ is made [29]. The `BAT-OK` signal is attached to the gate of an N-MOS. The N-MOS is connected between ground and the communications unit, so when the signal becomes high the communications unit will be disconnected, preventing any leakage current. One possible issue with this is that if the supply voltage drops below the threshold voltage of the N-MOS, the signal will not be able to close it properly. There is currently no real solution to this, however when this occurs the voltage should be sufficiently low that the communications unit will be entirely off, using no power.

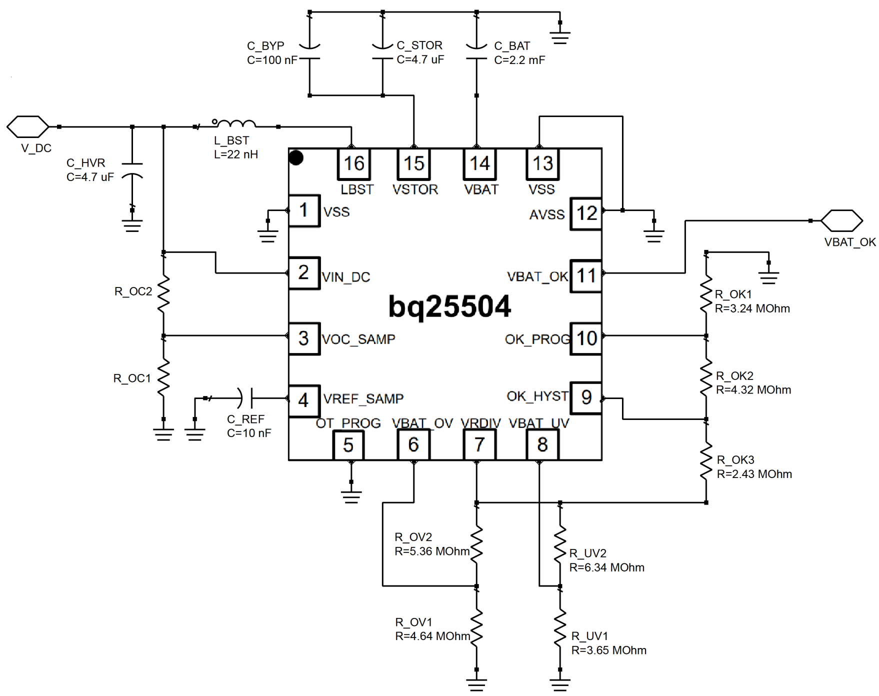

Figure 3.16: Schematic of a the BQ25504 with configuration components

The BQ25504 is also capable of varying its input impedance to optimize efficiency. This is done using another 10 MΩ resistor divider attached to the `V-SAMP` pin. Because it is not known at what output impedance the rectifier achieves highest efficiency a 10 MΩ potentiometer has been used as a voltage divider to allow this to be fine tuned after production.

Finally the BQ25504 has a built in over voltage protection. By attaching a final resistor divider to the `VBAT-OV` pin the over voltage threshold can be set. By using a 5.4 MΩ and a 4.6 MΩ resistor the threshold is set at 3.9 V. If this voltage is reached the chip will disable the boost converter and disconnect the load [29].

3.3. Storage

Since the energy harvester does not provide anywhere near enough power to allow for constant measurements/transmissions the energy needs to be stored somewhere. The following specifications have to be considered when designing a storage device. It needs to:

1. have a low leakage current
2. allow for constant charging/discharging
3. provide a high output voltage while storing a small amount of energy
4. have a long lifetime
5. easily be measured for SOC

The two options which come to mind are either a capacitor or some form of chemical battery. Chemical batteries usually offer much greater energy-density over capacitors. However because the amount of energy stored in this application is so small, this is not a factor at all. Chemical batteries also tend to have the edge in leakage current. However with the current topology the leakage through the reverse biased diodes and voltage dividers will be far greater then the leakage from the capacitor.

Capacitors handle being charged/discharged constantly a lot better. Traditional batteries do provide an advantage in lifetime, however due to the frequent charging and discharging this lifetime will be greatly reduced. In this particular situation a capacitor will likely outlast a battery, since it is operating at far below its rated maximum voltage at room temperatures. Lastly it is much easier to determine how much energy is stored in a capacitor using simple electronics. Batteries are designed to output the same voltage regardless of how much energy is stored. This makes determining the SOC using a voltage sensor much more difficult. With a capacitor the voltage is directly related to the amount of energy stored in the capacitor. For these reasons it has been decided to use a capacitor as the main storage device [30].

The sensor readout and transmission require 4 mJ amount of energy [10]. The power specifications of the sensing and communication unit are given in Tab. 3.2.

Table 3.2: Sensing and communications unit power requirements

Parameter	**Value**
V_{min}	2.7 V
V_{max}	3.7 V
$E_{required}$	4 mJ

$$E = \frac{1}{2}CV^2 \tag{3.6}$$

The energy stored in a capacitor is given by eq. 3.6. In order to store 4 mJ amount of energy between V_{min} = 2.7 V and V_{max} = 3.7 V a capacitor of at least C_{store} = 1.25 mF is required.

4

Prototyping and Validation Results

In order to verify the design made in chapter 3 it will need to be synthesized. An overview of the design of the whole subsystem can be found in Appendix C. Initially, a circuit was built using a prototyping board using common through-hole components. While this worked at low frequencies it quickly became apparent that this would not suffice for radio-frequency inputs. Through-hole capacitors tend to only function up to about 30 MHz, after which they display characteristics similar to an inductor. Another issue is that the pads on a prototyping board are relatively close together, and there are a lot of unused pads. These pads create a lot of parasitic capacitance, which can greatly influence the operation of the circuit at high frequencies. Lastly most of the components that are able to operate at high frequencies tend to be surface mount, making soldering them on a prototyping board difficult at best. For these reasons it has been decided to instead produce a PCB.

4.1. PCB Design

When designing the PCB a few things have to be taken into account[1]. First of all it is important that the components that handle high-frequency signals are physically close to each other. The working frequency of this system is roughly 850 MHz, meaning that the wavelength λ is about 35 cm. As a rule of thumb transmission line effects start when a line is longer then 10% of the wavelength, meaning that in order to avoid these effects the components need to be placed within 3.5 cm of the antenna connector [12]. These components include the matching network[2] and the diodes/capacitors from the rectifier. After that all signals are DC, so no transmission line effects should occur.

Additionally it was deemed wise to be able to separate the different subsystems from each other to be able to test all the subsystems apart. The rectifier is connected to the DC/DC-converter using a header, which can be easily disconnected to test the rectifier with an arbitrary load. The same is done for the communications unit. These headers also allow for certain parts to be redesigned after production of the PCB. Certain parts where unable to be simulated or otherwise verified beforehand. Namely the DC/DC-converter is an unproven design. Since only the high frequency parts of the circuit have to explicitly be put on a PCB it is possible to redesign and rebuild the other parts on a prototyping board without having to reorder a PCB. This prototyping board can then be slotted in using the header pins. The final PCB layout can be found in figure 4.1 and a more detailed PCB-design can be found in Appendix E.

[1] While this section focuses on the PCB design for the conversion unit, the designed PCB contained the other subsystems as well, and design decisions related to this are mentioned as well.

[2] In this section the design of the final product is used, meaning that the matching circuit has been merged with the matching circuit of the antenna. In the previous chapter the rectifier was matched to a fictitious 50 Ω antenna.

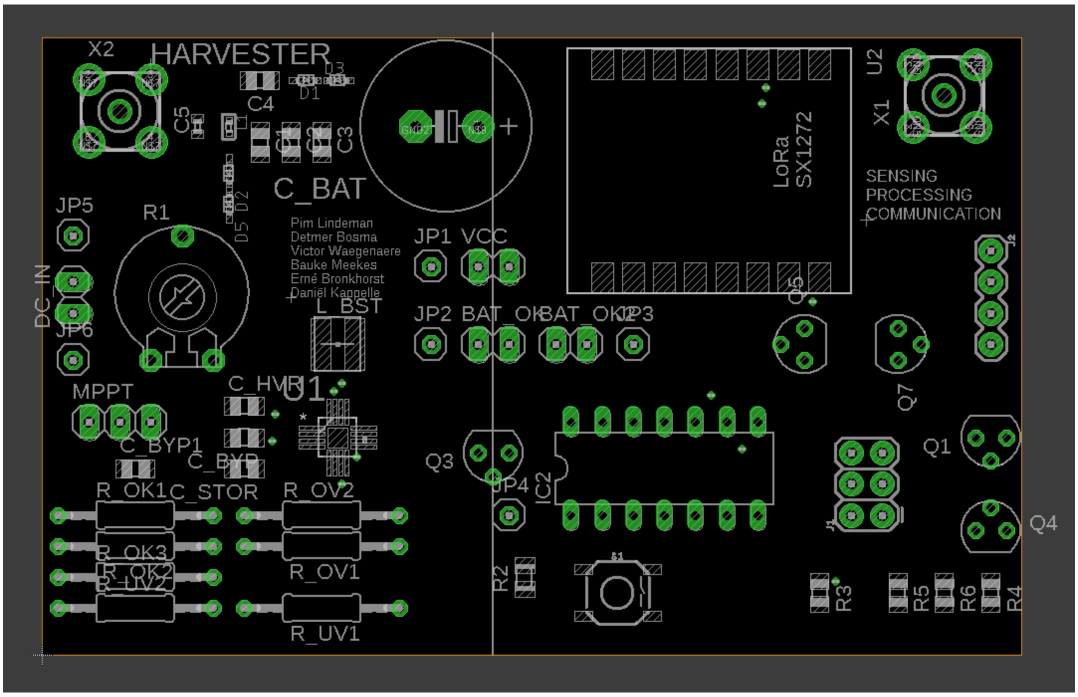

Figure 4.1: Final PCB layout of the entire system

4.2. Component selection

Since parts of the circuit are operating at very high frequencies selecting the components is not always trivial. Extra care has to be taken when selecting the components of the matching circuit and the rectifier. As previously mentioned most capacitors start showing behaviour similar to inductors at frequencies above 30 MHz, therefore special high-frequency capacitors where chosen. Ideally the capacitor in the matching circuit would be a variable capacitor. Sadly variable capacitors where not available in the desired range. It was considered to put a capacitor in series with a larger variable capacitor to reduce the combined value, but this was ultimately abandoned as this would result in additional losses and increased complexity.

Inductors are also not necessarily constant in value as the frequency changes, and this has been taken into account when selecting the inductor for the matching network. A conscious effort has been made to not order parts smaller then the 0805 package size, as soldering smaller parts to the PCB is very difficult without specialized tools. Only the diodes are in a smaller package, since a very specific diode was required and these where only available in one package size (for more on the selection of this diode, see section 3.1.1). The resistors in the resistor dividers for the DC/DC-converter are all through-hole resistors. This makes them easy to solder and, more importantly, easy to swap out for a different value if the thresholds for the DC/DC converter turn out to not be set properly. The same goes for the storage capacitance. If in practice it turns out that this needs to be larger or smaller it can be replaced easily. A full list of all used components can be found in Appendix D.

In section 3.1.6 the matching circuit was designed to a 50 Ω antenna, as result a 27.5 nH inductor in parallel and a 0.754 pF capacitor in series. In order to match the subsystem to the antenna, the impedance of the antenna was measured by a vector analyzer. The impedance of the antenna is equal to 87-j18.5 Ω en therefore a 26 nH inductor in parallel and a 0.9 pF capacitor in series are used to match the subsystems.

4.3. Testing

Once the PCB had been built it was thoroughly tested for functionality. Because of the modular design it was possible to test the subsystems separately.

4.3.1. Rectifier

The output of the rectifier was tested while the DC/DC-converter was still attached, but without the communication unit. The output voltage was measured using an oscilloscope. When the device was just laying on a table no detectable output was present. Whenever a phone was put in close proximity (roughly 5 cm) of the antenna occasional spikes in the output voltage where made visible on the oscilloscope. These spikes would be up to 200 mV in amplitude, depending on the distance between the phone and the antenna and the type of phone being used. When a phone would be called when close to the antenna the voltage would rise to a much higher voltage, and remain there. Depending on the type of phone being used the voltage could spike as high as 2 V. An example of this can be seen in figure 4.2. The dip at the end of the graph is caused by the phone being moved away from the antenna. On a separate voltmeter the output voltage could be seen to be rising as well, but this was not visible on the oscilloscope as the timescale was too small.

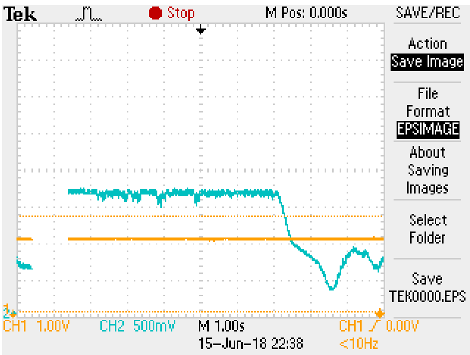

Figure 4.2: The output voltage as a phone in close proximity of the antenna was being called. The blue line represents the output of the rectifier, and the yellow line is the output of the DC/DC converter. Here the x-axis represents the time (1 sec per square) and the y-axis represents the voltage (1.0 V per square for CH1, 500 mV per square for CH2)

The input impedance of the entire circuit as seen from the antenna input was also measured using a vector network analyzer. The measurements where taken from 800 MHz to 900 MHz at -10, -20, -25 and -30 dBm. The -25 dBm results can be seen in figure 4.3, the others can be found in Appendix F. The impedance at 845 MHz and -25 dBm - the conditions at which matching should occur - is 6.889 -40.54j Ω. More information on the network analyzer used can be found in [11].

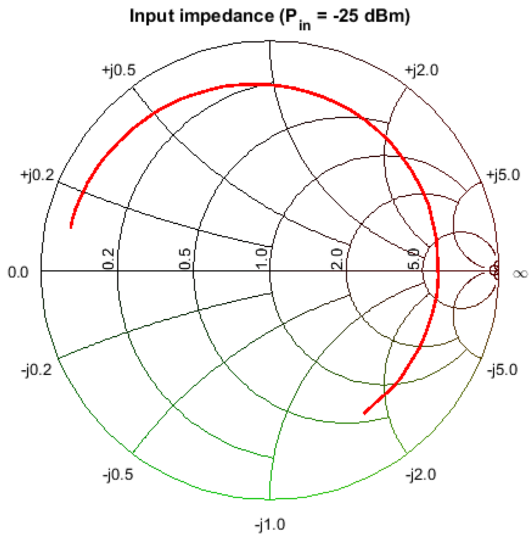

Figure 4.3: Input impedance from 800 to 900 MHz at -25 dBm as measured by a vector analyzer.

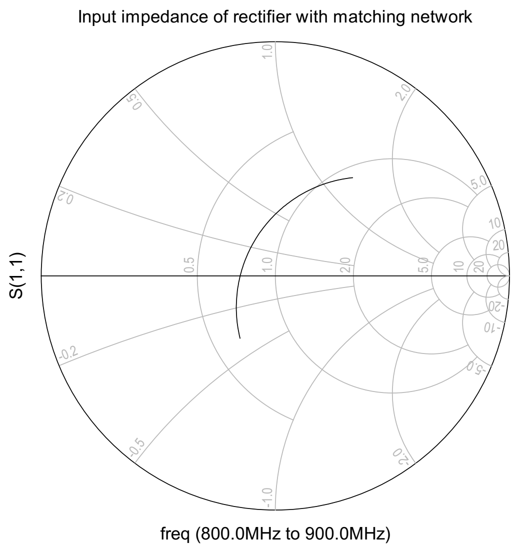

Figure 4.4: Input impedance from 800 to 900 MHz at -25 dBm as simulated with ADS

It was not possible to determine at what input power level would result in what output voltage for the rectifier. The antenna input could not simply be connected to an 845 MHz oscillator, as all available oscillators had an output impedance of 50 Ω, and the input impedance of the rectifier has been matched to the impedance of the antenna. Therefor it was not possible to determine the total efficiency of the rectifier.

4.3.2. DC/DC-converter

The `BAT OV` and `BAT OK` trigger and hysteresis thresholds of the DC/DC-converter were also tested. This was done by disconnecting the rectifier and communications unit and supplying the DC/DC converter directly using a power supply. The power supply was set to 400 mV and current limited at 0.6 mA to simulate the power coming from the rectifier. The voltage across the storage capacitor was measured, as well as the `BAT OK` signal. The `BAT OK` signal remained equal to a digital 0 until the storage capacitor reached 3.76V, at which point the signal became high, indicating that a measurement could be taken. Since the communication unit was not connected no temperature measurement was actually taken and the voltage in the capacitor continued to rise. Once the voltage in the capacitor reached 4.05 V it would stop increasing, indicating that the converter went into over-voltage protection. When the capacitor was discharged using a 10 kΩ resistor the `BAT OK` signal would go low again once a voltage of 2.72 V was reached. A quick overview of the specified thresholds and actual threshold can be found in Tab. 4.1.

Table 4.1: Specified and measured threshold voltages.

Signal	**Specified**	**Actual**
`BAT OK` trigger	2.8	2.72
`BAT OK` hysteresis	3.7	3.76
Overvoltage Protection	3.9	4.05

However issues would arise when the input current was higher then 0.6 mA. The overvoltage threshold would vary randomly between 3 and 4 volt, and the `BAT OK` signal would oscillate between high and low when a voltage of 3.6 V was reached, instead of switching on and off instantly.

The input voltage at which the DC/DC converter should start operating is specified at 330 mV during a cold start and 80 mV during normal operation [29]. However this turned out to not necessarily be true in practice. When the storage capacitor was empty a voltage of 380 mV was required to start charging the capacitor. The charging current would be about 1 mA, while the charging voltage would be the same as the supply voltage.

Once the capacitor reached a voltage of 1.7 V the the DC/DC-converter would switch to its normal operation mode with its main boost charger turned on, at which point the charging current would increase significantly, going up to 6 mA (the maximum current dialed into the power supply). The voltage at the input of the DC/DC would always be about 75% of the voltage dialed into the power supply, regardless of the settings of the current limiter. During normal operation it would sometimes be possible to lower the input voltage to as low as 60 mV. However often charging would stop seemingly at random. Whenever this occurred the voltage would need to be increased again to about 360 mV, at which point charging would resume. Once charging had resumed the voltage could be dropped again. While charging a current would flow into the converter at very low voltages, at least 130 mV input voltage was required to overcome the current leaking from the capacitor. It should be possible to regulate the voltage at the input of the DC/DC-converter using the MPPT-tracking feature of the DC/DC-converter. However enabling this and playing around with the potentiometer that regulates this had no effect on the input voltage (or current for that matter).

In order to determine the efficiency of the DC/DC converter a 370 mV signal current limited at 1 mA was applied to the input of the converter. A timer was started once the voltage at the output read 2 V. The voltage was left to increase up to 3.7 V, which took 84 seconds. So during this time a 2.2 mF capacitor was charged from 2 V to 3.7 V, which takes 10.7 mJ of energy. The voltage at input of the converter was 280 mV and it was drawing the full 10 mA for 84 seconds, which equates to 23.5 mJ of energy flowing into the converter. This results in an efficiency of 45%. According to the data sheet of the DC/DC-converter this efficiency will be better with higher input voltages, depending on the available ambient RF energy at the antenna.

4.3.3. Storage

The storage capacitor was tested for input leakage current by charging it up to 2.8 V and allowing it to discharge naturally to 2.5 V. The rectifier was connected, but the antenna was not so no harvesting could occur. It takes 29 minutes to discharge the capacitor 0.3 V, with a voltmeter attached to the capacitor. The voltmeter itself has an impedance of 11 MΩ, which is likely what caused the majority of the leakage current. While the antenna was disconnected, a voltage source was connected to the DC/DC-converter and so the voltage across the storage capacitor was increasing. It takes 62 seconds to charge the capacitor from 2.8 V to 3.7 V with a input voltage of 360 mV, which is the range of the `BAT-OK`-signal being high.

The communications unit was also tested using the capacitor as a power supply. The communications unit would be able to perform 2 measurements before it would be shut down by the `BAT OK` signal.

5 Discussion

In chapter 4 the results of the testing of the prototype were presented. In this chapter these results will be analyzed and it will be discussed whether the requirements of chapter 2, especially the requirements of the subsystem, are met or not.

5.1. Rectifier

While testing the rectifier, the conclusion can be made that the subsystem is able to convert the input voltage to a DC output voltage. The chosen Schottky diodes and capacitors operate properly at high input frequencies between the 800 MHz and 900 MHz. Therefore requirements **4-1** and **4-9** are both met. In chapter 4 it was mentioned that it was not possible to directly measure the output voltage for a given input power. However it is unlikely that the rectifier met its power requirement. In [11] is suggested that peaks up to -25 dBm should be available at all times, but these peaks where not visible at the output of the rectifier. Therefore requirement **4-4** has not been met.

For maximum power transfer to the load a matching circuit had to be designed and therefore the input impedance of the subsystem should be known. The matching circuit between the antenna and the rectifier was based on results from ADS simulations. The measurements of the input impedance of the subsystem (with the matching circuit) can be seen in Fig. 4.3 on page 17. The input impedance of subsystem at frequency 845 MHz is equal to 6.89-j40.54 Ω and the impedance of the antenna is equal to 87-j18.5 Ω. Therefore the matching between the subsystems is very bad, resulting in poor power transfer and the requirement **4-8** has not been met.

The actual impedance is a far cry from what was simulated using ADS. Most notable is the increased frequency dependency and increased imaginary part. This can largely be explained by the fact that ADS does not take the inter-trace capacitance into account. The only capacitance considered in the simulations are the diode capacitance and the intentionally placed capacitors. In reality however there exists capacitance between the traces on the PCB. Also while the traces on the PCB in the high-frequency parts where intentionally left short, transmission line effects will still take place. This also results in additional imaginary components in the input impedance. The significant miss-match between the simulation and reality can be seen in Fig. 4.3 and Fig. 4.4 on page 17.

5.2. DC/DC-converter

While the DC/DC-converter worked well in most circumstances, it was far from perfect. When ~370 mV was available at the input, the converter would always produce a correct output. However when less was available the output was inconsistent at best. As previously mentioned the converter would only start working when it reached a 370 mV input voltage, after which the input would be able to drop as low as 60 mV while still supplying an output. However charging would often stop seemingly at random. While the available power is often present in spikes [11], these spikes will rarely go above 370 mV, even with perfect matching and a loss-less matching circuit. In its current form an output of more then 2.7 V from the capacitor cannot be guaranteed, as the amount of power needed to overcome the leakage from the capacitor is more then is generally available. Therefore requirement **4-2** has not been met.

Dependent on the available ambient RF energy it is hard to measure the time needed to charge the capacitor until 4 mJ is stored using the antenna as power source. Testing the subsystem with the voltage source as input fixed at 360 mV, the energy level was achieved in approximately 2 minutes. This energy level is achieved if the voltage across the capacitor is equal to 3.76 V and at this point the `BAT OK` signal will change from a digital 0 to a digital 1, which follows the voltage across the capacitor. After the communication module will send a data measurement unit, the voltage will drop to 3.3 V. Therefore the requirements **4-6** and **4-7** are met.

While the thresholds for the `BAT OK` signal are within the bounds set by the requirements, the overvoltage protection is not. When supplying the converter with a low current the overvoltage protection would kick in at 4.05 V, which is significantly higher then the specified 3.9 V and is high enough that it could potentially damage the communications unit. This threshold is set by a voltage divider consisting of a 5.4 MΩ and a 4.6 MΩ resistor. However since these specific values of resistors where not available a 5.1 MΩ and 4.3 MΩ resistor where used instead. This shifted the threshold up. While the device should theoretically never go into overvoltage protection, it is still something that should be considered in future work. Therefore requirement **4-3** has not been met.

No adequate explanation has been found for the fact that the overvoltage threshold would be inconsistent when presented with an input current of more than 0.6 mA. It shouldn't however pose an issue as these input currents would be very rare during normal operation, and the threshold has only been observed to go down, not up. This would result in functionality potentially temporarily being halted, but won't result in permanent damage to electronics.

5.3. Storage

The storage performed as expected. The capacitor could have been made smaller, as it is currently possible to do two measurements without needing to recharge. Reducing the size of the capacitor would make charging it more quickly, allowing the measurements to be better spaced out over time. The leakage from the capacitor was within bounds, as (if the rectifier met its specifications) would easily be able to be overcome. Therefore requirement **4-5** has been met.

6 Conclusion

The designed system is able to harvest RF energy from the GSM-band (800-900 MHz) and to convert this to an usable output voltage. In order to rectify this signal a full-wave Greinacher rectifier is used with a Schottky diode which operates properly with high frequencies and has a very low threshold voltage (~ 150 mV). Simulations with Advanced Design System (ADS) indicated that the SMS7630-diode was best to use on 845 MHz. The rectifier converts the AC-signal to DC and doubles the input voltage minus two times the threshold voltage of the diode. It turns out using a single stage rectifier is most efficient with input powers lower than -25 dBm.

In order to achieve maximum power transfer to the load the subsystem has to be matched to the antenna. To reach a high output voltage a high input voltage is needed and so it is favorable to have a high input impedance. It appeared to be that a single stage rectifier has the highest input impedance for low input powers. The input impedance is equal to 82+j314 Ω, resulting in a matching circuit consisting of a parallel 26 nH inductor and a 0.9 pF capacitor in series. The matching circuit was designed at a frequency of 845 MHz and boosted the voltage to 360 mV with an input of -25 dBm. A DC/DC-converter is used to convert this 360 mV to a 3.3 V output voltage, which is connected to a 2.2 mF capacitor for charging. The DC/DC-converter gives a signal to the communication module whether enough energy is stored in the capacitor, which must be 4 mJ, equal to 3.7 V across the capacitor.

This subsystem is printed together with the communication module on a PCB. The rectifier and the DC/DC-converter are tested separately from eachother. From the test results it can be concluded that the produced prototype did not meet the requirements, although the basic techniques that could be used to harvest ambient RF energy have been proven. The main issue was that the ambient RF radiation would not induce enough voltage to overcome the threshold voltage of the diodes. However when enough energy was present the rectifier was shown to work, even when only short pulses of energy where available.

The DC/DC converter, while not quite meeting the requirements, still showed promise as a concept. The start-up input voltage was higher then expected, but not so high that reaching it would be theoretically impossible using only ambient power. Additionally the converter would continue to work at low input voltages. Even though this was unreliable, it still shows potential for the device to work at very low input powers.

The matching circuit did not perform well at all. The output of the antenna was not matched to the circuit. This is partially responsible for the low output voltages at low power levels. Determining the input impedance using ADS was simply not accurate enough to design a proper matching circuit.

6.1. Recommendation

In future it would be recommended to use a better method to determine the input impedance of the rectifier, so a better matching network can be made. This can easily be done by producing just the rectifier (without matching) on a PCB and using a vector network analyzer to determine the input impedance. This method takes int account all off the parasitic effects present in real world electronics. This data could then be used to design a more effective matching circuit. Additionally the matching circuit should contain a variable element of some sort, allowing the input impedance to be fine-tuned after production. One consideration that could be made is the match the system to 50 Ω, and use a 50 Ω antenna. This allows the system to be tested using conventional oscillators as a substitute for an antenna.

Not many improvements can be made to the rectifier circuit. Some more research could be done in fine-tuning the values of the capacitors. These are currently not the cause for a lot of the losses, but a small improvement in efficiency could still be possible. The only way to improve the efficiency in a meaningful way would be to find even lower threshold diodes. Research is currently underway into designing very low threshold CMOS circuits, however these are currently not significantly better then Schottky diodes [31].

Not a lot of improvements can be made regarding the DC/DC-converter either. More research should be done in the MPPT of the converter, as this should be able to improve the efficiency of the device. Also steps should be taken to make it more reliable, even when presented with lower input power. This can potentially be done by varying the size of the input capacitor. Research could also be done in increasing the resistor values in the voltage dividers. This could reduce leakage from the storage device, but choosing these values too large may make the thresholds unstable.

A

Multiple stages

A.1. Circuits

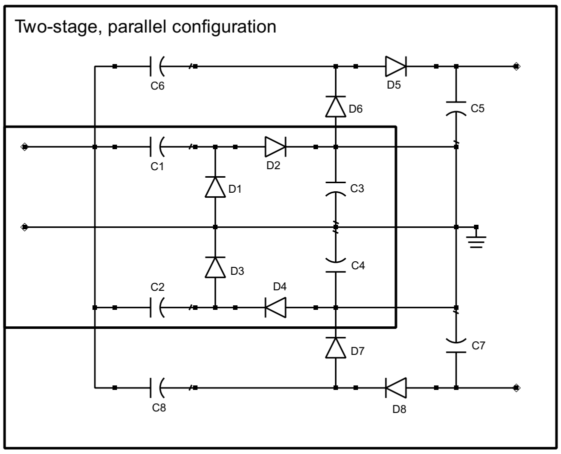

Figure A.1: Two-stage rectifier with parallel configuration

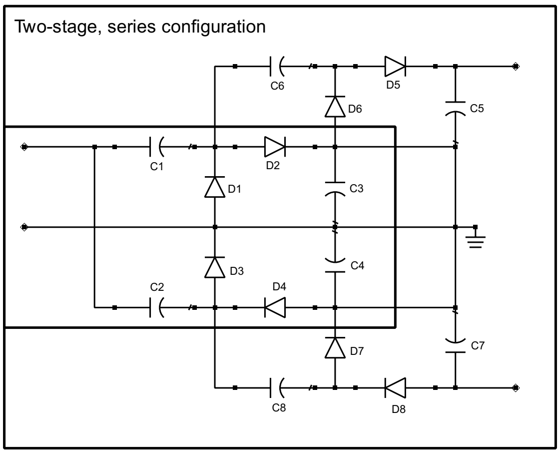

Figure A.2: Two-stage rectifier with series configuration

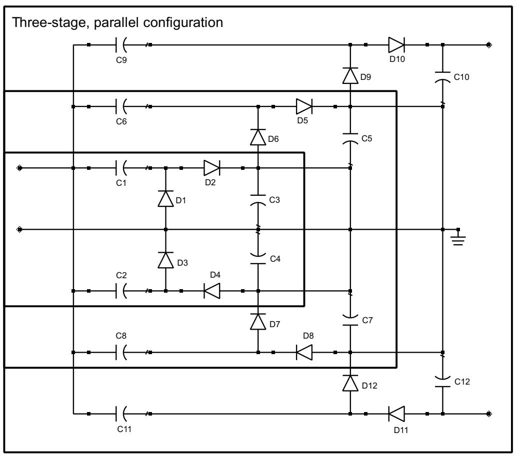

Figure A.3: Three-stage rectifier with parallel configuration

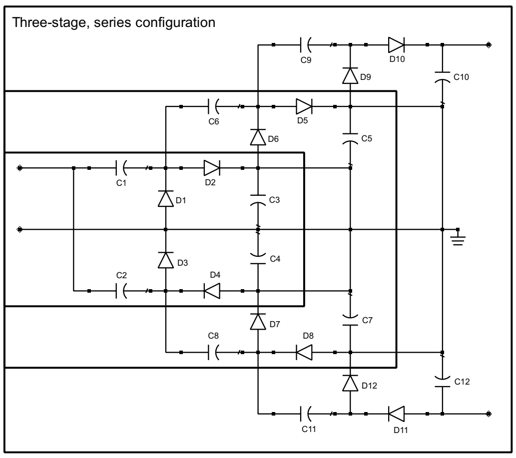

Figure A.4: Three-stage rectifier with series configuration

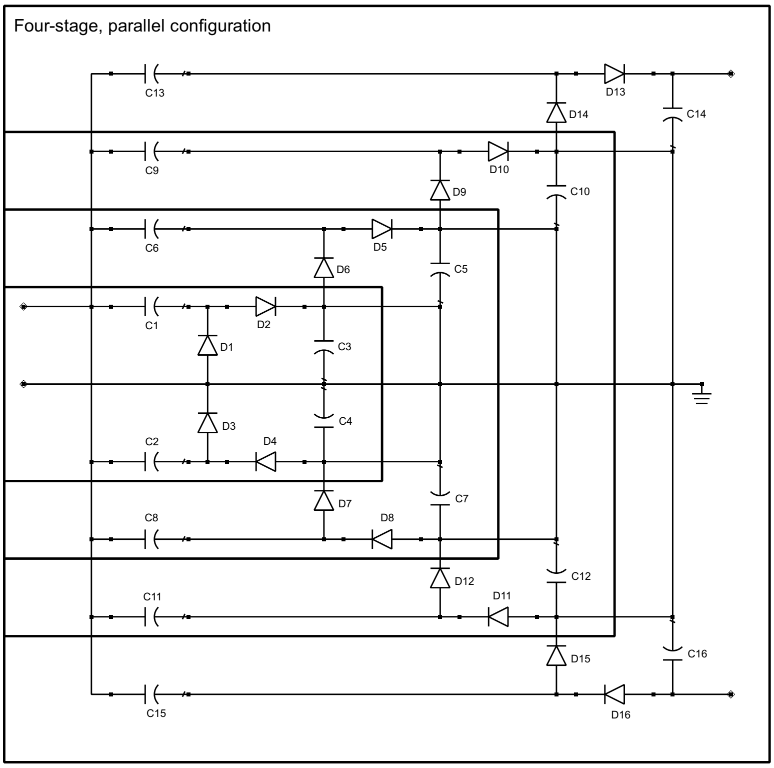

Figure A.5: Four-stage rectifier with parallel configuration

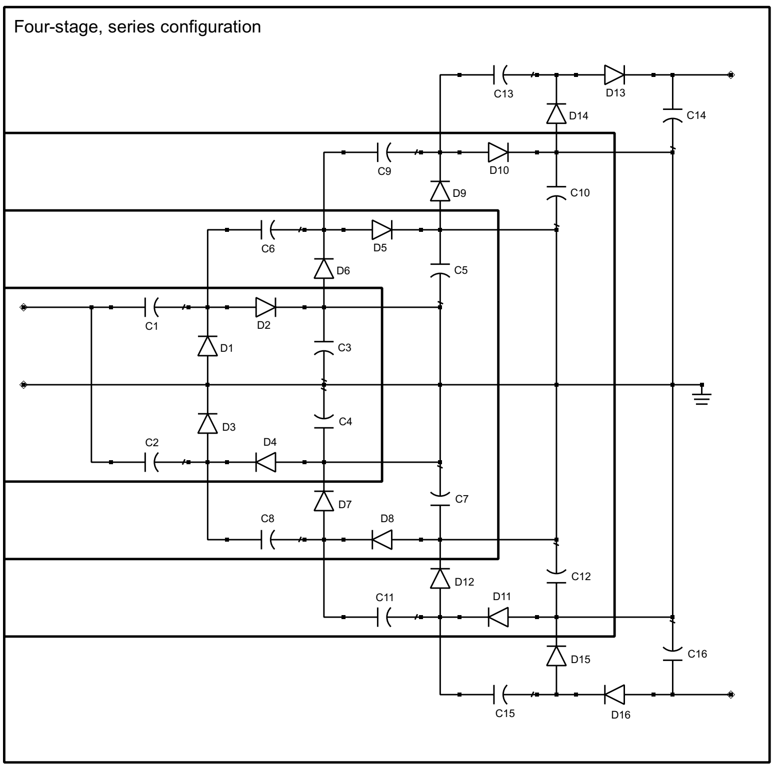

Figure A.6: Four-stage rectifier with series configuration

A.2. Input impedance for both configurations

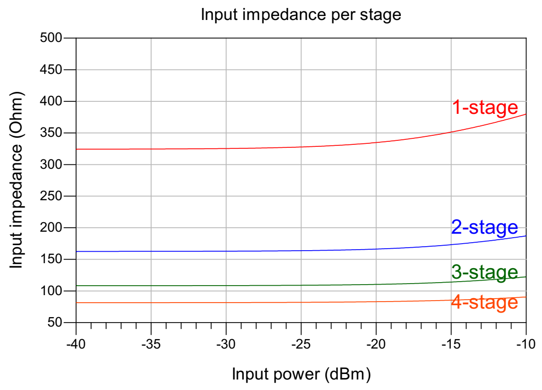

Figure A.7: Input impedance per stage with parallel configuration. It shows the 1-stage rectifier has the highest impedance

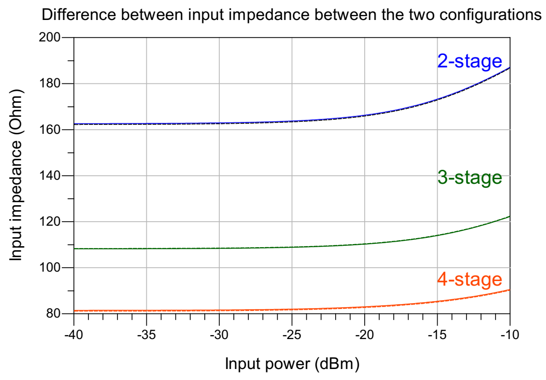

Figure A.8: Input impedance per stage with both configurations (parallel config.: solid line; series config.: dotted line)

A.3. Output voltage for both configurations as function of time

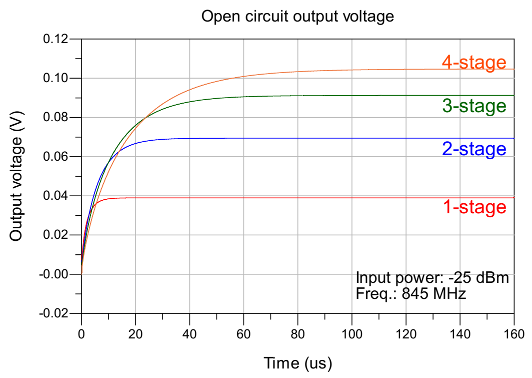

Figure A.9: Open circuit output voltage per stage with parallel configuration. All rectifiers are unmatched.

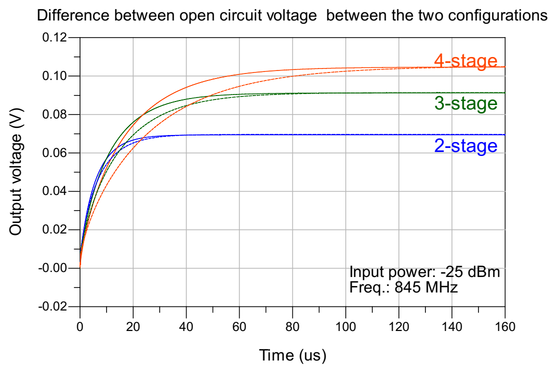

Figure A.10: Open circuit voltage with both configurations (parallel config.: solid line; series config.: dotted line)

A.4. Output voltage for both configurations as function of input power

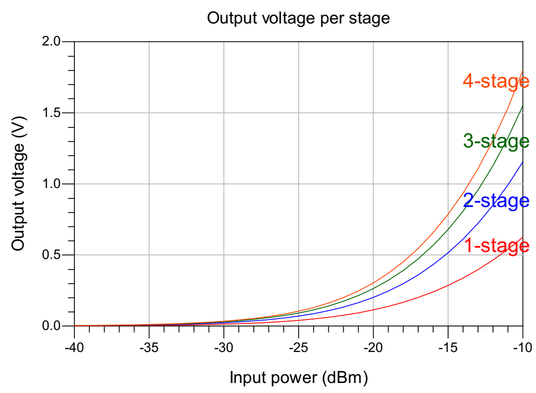

Figure A.11: Output voltage per stage with parallel configuration. All rectifiers are unmatched.

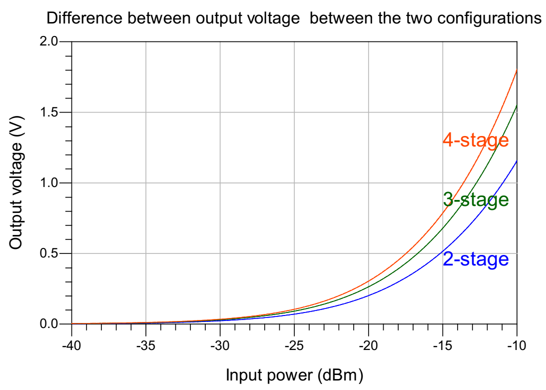

Figure A.12: Output voltage per stage with both configurations (parallel config.: solid line; series config.: dotted line)

B

Matching circuit

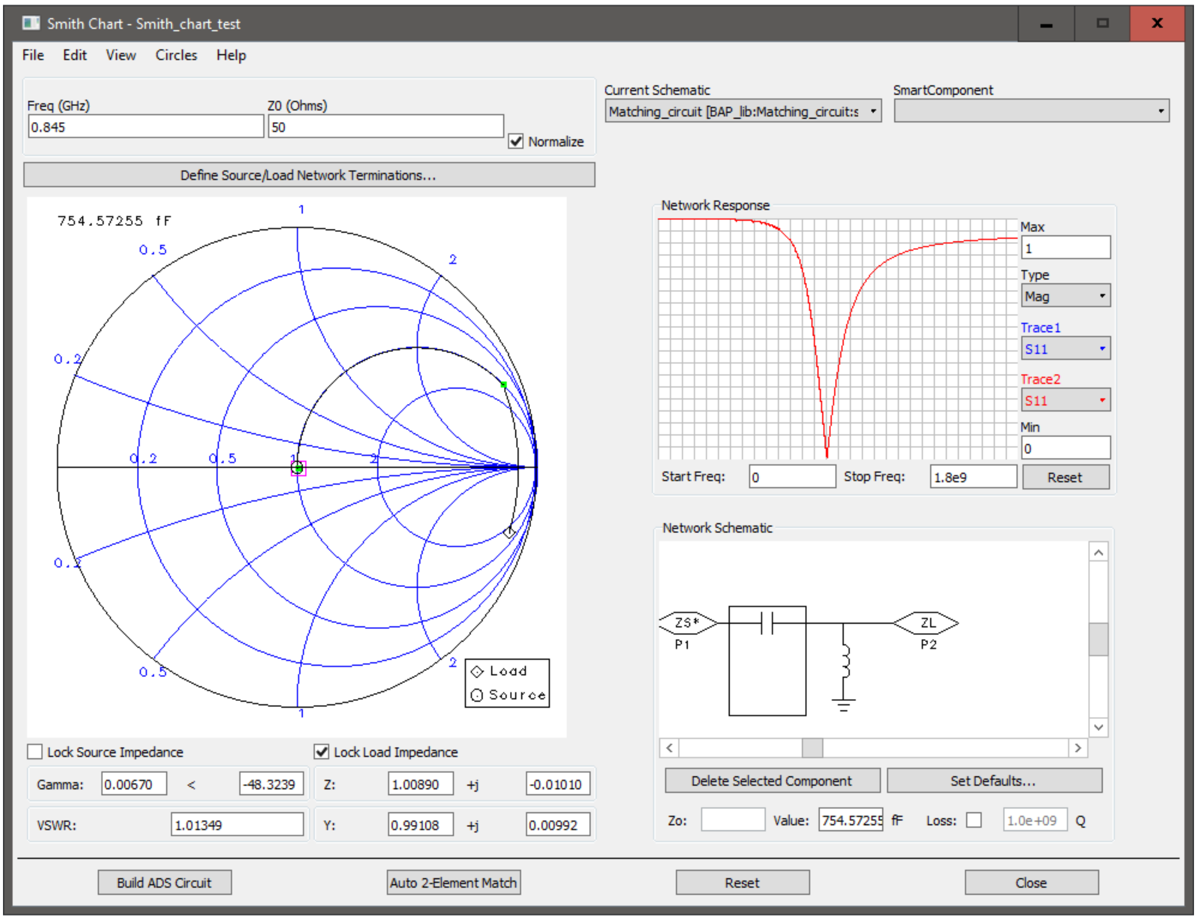

Figure B.1: Smith Chart of the matching circuit. The inductor and capacitor shift the input impedance to the midpoint of the graph, which is equal to 50 Ohm.

C
Full subsystem

On the next page the full circuit with matching circuit, single stage Greinacher rectifier and the DC/DC-converter can be seen.

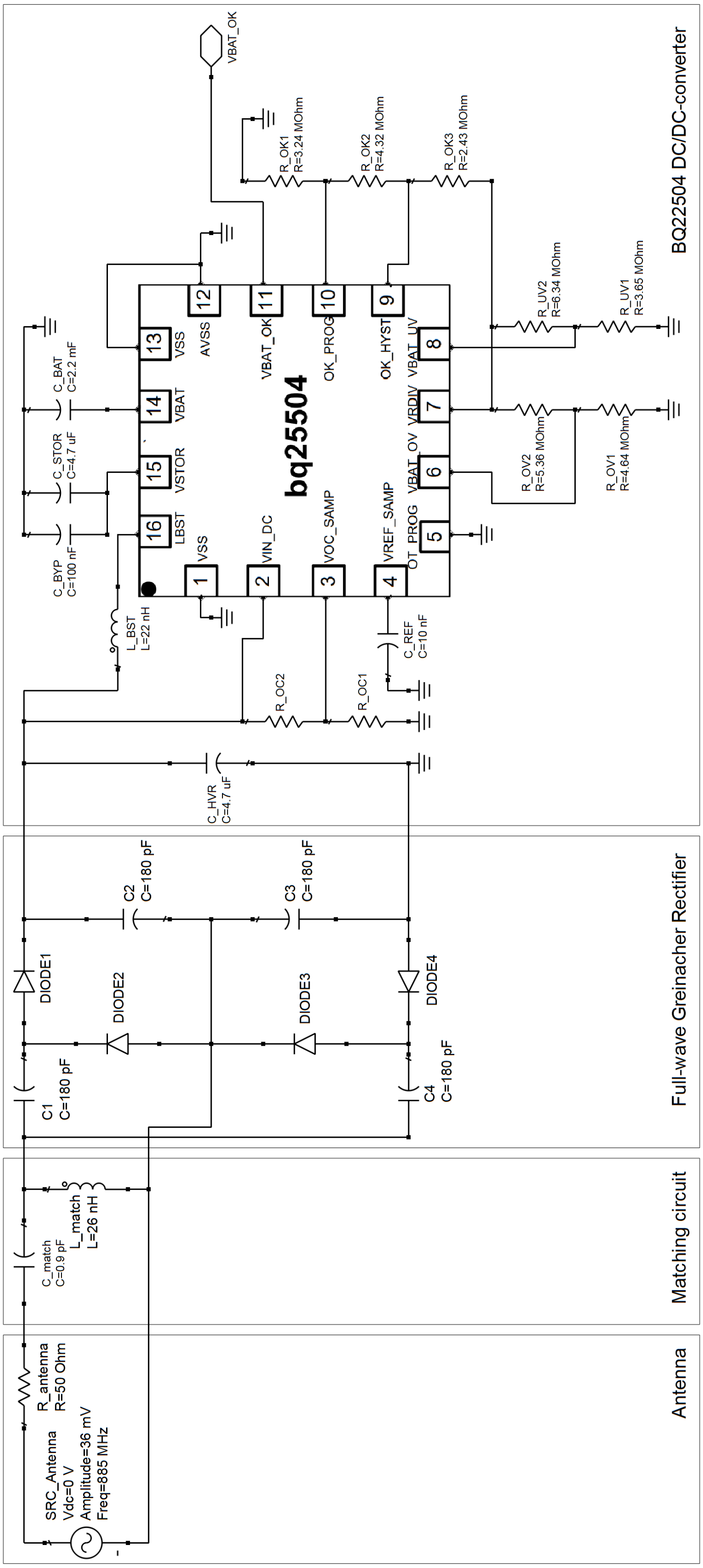

Figure C.1: The full circuit with matching circuit, single stage Greinacher rectifier and the DC/DC-converter.

D

Parts list subsystem

Table D.1: List of all parts used in the whole system

Ordercode	Aantal	Prijs	Subtotaal	Beschrijving
1654645	1	€ 6,50	€ 6,50	SMA adapter
2112448	3	€ 3,09	€ 9,27	SMA connector
2116082	1	€ 0,34	€ 0,34	Inductor 26 nH (matching)
2809739	1	€ 0,05	€ 0,05	Capacitor 0.9 pF (matching)
1753779	4	€ 0,46	€ 1,84	SMS7630 Schottky diode
1227550	1	€ 0,71	€ 0,71	Potentiometer 10M through-hole
2362111	2	€ 0,23	€ 0,46	Capacitor 4u7 0805
2211001	1	€ 0,32	€ 0,32	Capacitor 0.1 uF 0805
1457736	1	€ 0,32	€ 0,32	Capacitor 0.01 uF 0805
1822600	1	€ 0,54	€ 0,54	Capacitor 2.2 mF
1885453	4	€ 0,33	€ 1,32	Capacitor 180 pF 0805
-	3	€ 0,00	€ 0,00	MOSFET transistor, N-channel
9469273	1	€ 0,09	€ 0,09	5M1 res through-hole
9468730	1	€ 0,06	€ 0,06	4M2 res through-hole
9469834	1	€ 0,08	€ 0,08	6M2 res through-hole
9467955	1	€ 0,08	€ 0,08	3M6 res through-hole
9466894	1	€ 0,08	€ 0,08	2M4 res through-hole
9468730	1	€ 0,06	€ 0,06	4M3 res through-hole
9467947	1	€ 0,05	€ 0,05	3M3 res through-hole
1653018	2	€ 0,03	€ 0,06	51k res 0805
2144306	1	€ 5,32	€ 5,32	DC/DC-converter bq25504
1890602	1	€ 1,40	€ 1,40	Inductor 22uH
3801305	1	€ 0,12	€ 0,12	Reset-button
2500100	1	€ 18,64	€ 18,64	LoRa module
-	1	€ 4,27	€ 4,27	Temperature Sensor Breakout - TMP102
1699394	1	€ 0,97	€ 0,97	AtTiny 24A
Totaal			**€ 52,94**	

E

Full PCB-design

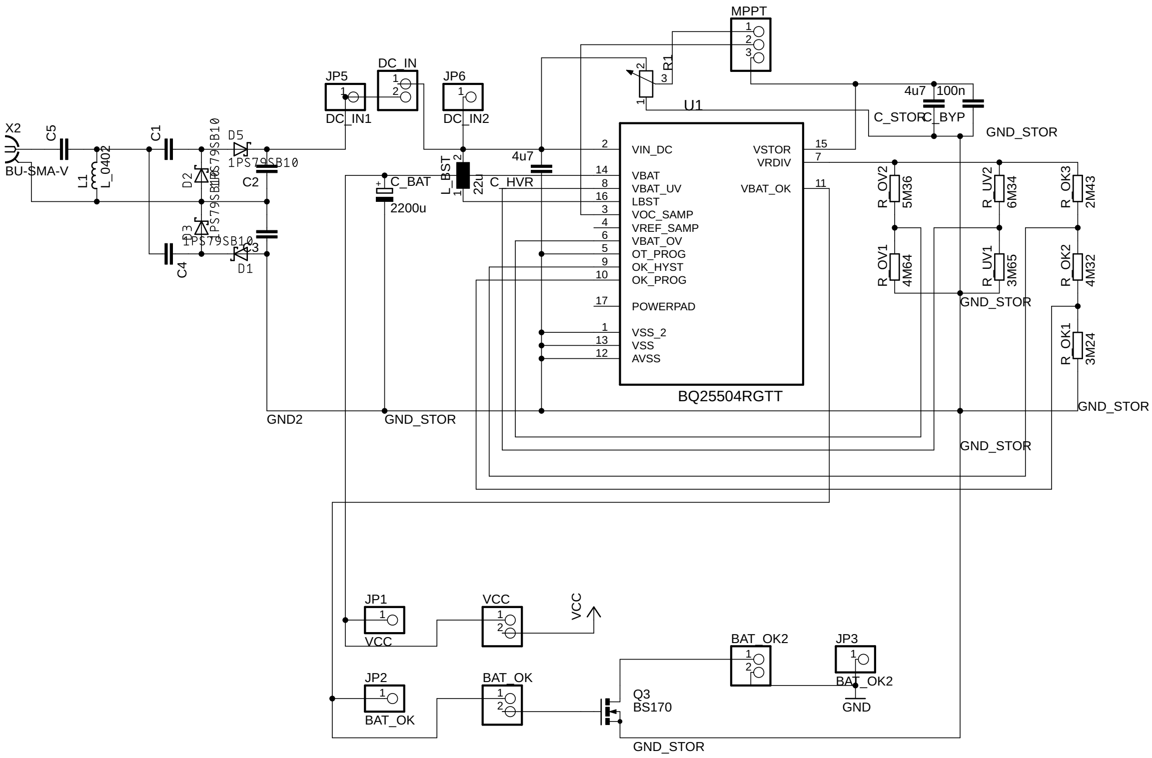

Figure E.1: The PCB design of the antenna and rectifier subsystem

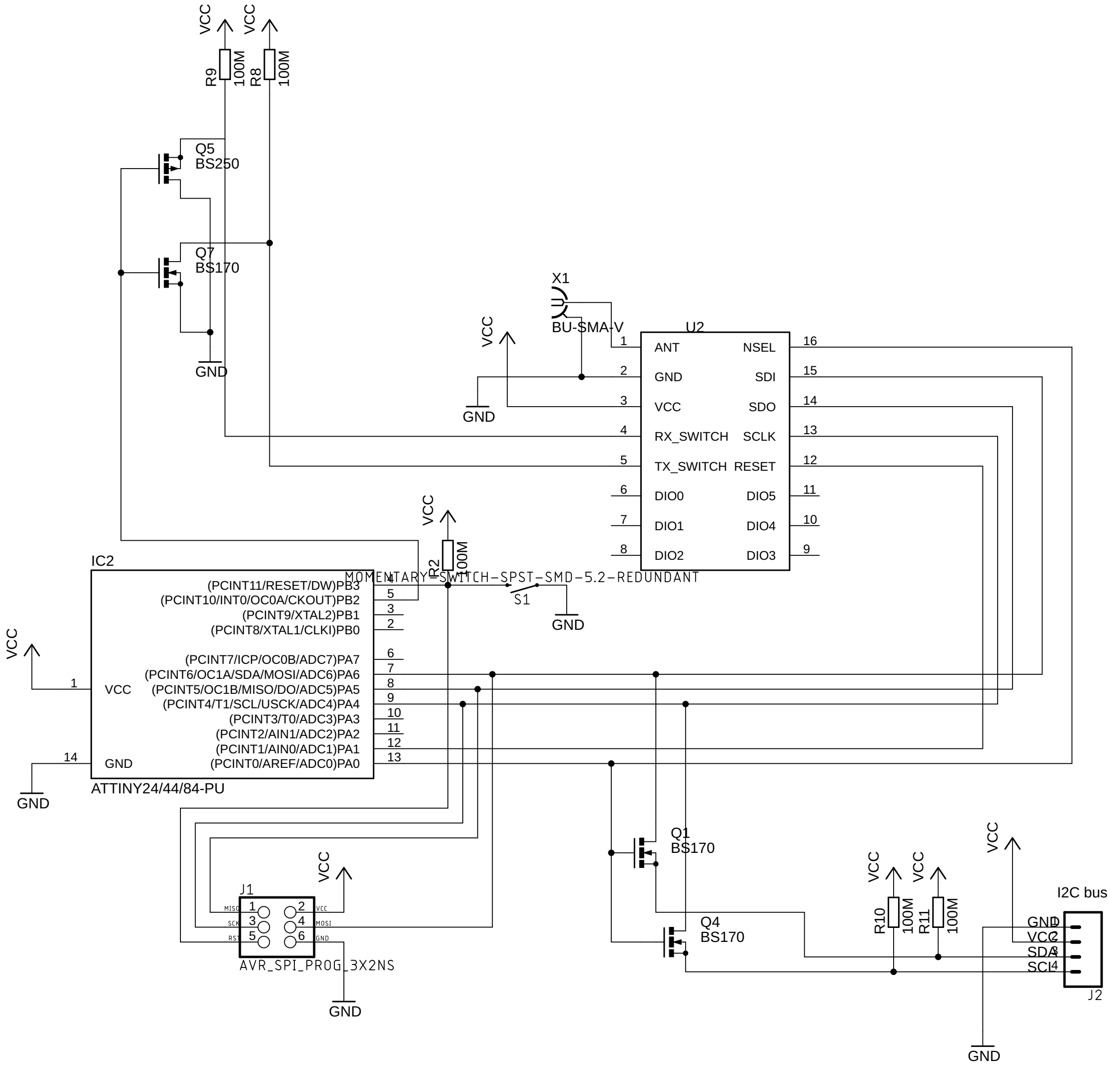

Figure E.2: The PCB design of the sensing and communication subsystem

F

Measured input impedances

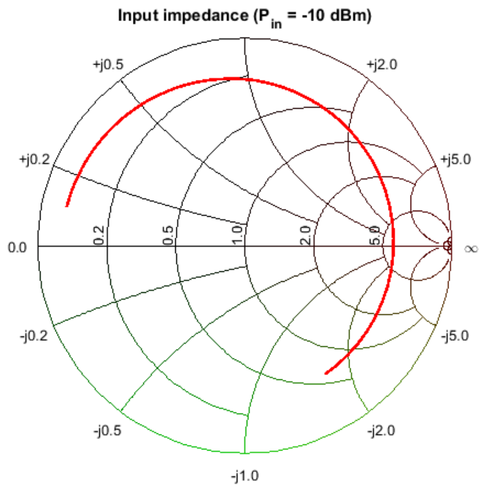

Figure F.1: Measured input impedance from 800 MHz to 900 MHz at -10 dBm measured by a vector analyzer.

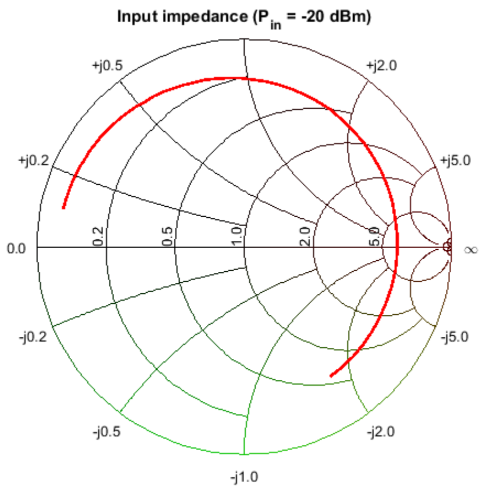

Figure F.2: Measured input impedance from 800 MHz to 900 MHz at -20 dBm measured by a vector analyzer.

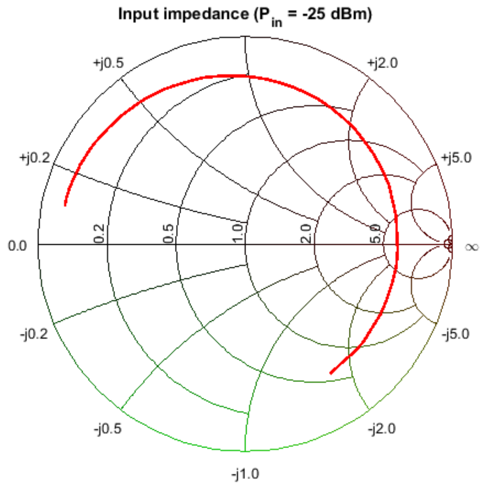

Figure F.3: Measured input impedance from 800 MHz to 900 MHz at -25 dBm measured by a vector analyzer.

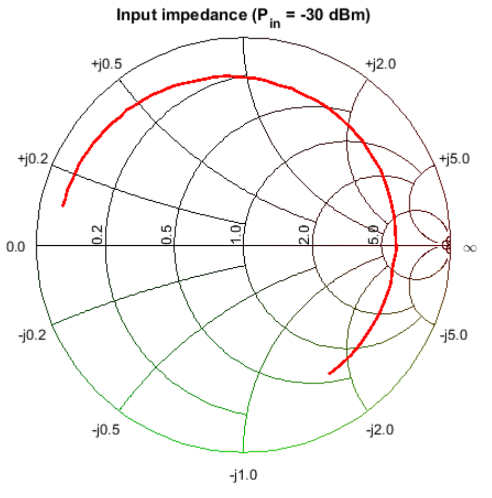

Figure F.4: Measured input impedance from 800 MHz to 900 MHz at -30 dBm measured by a vector analyzer.

Bibliography

[1] T. Sun, X. Xie, and Z. Wang, *Wireless Power Transfer for Medical Microsystems.* Springer Science & Business Media, 2013.

[2] S. Ashley, "Wireless charging: Pulling the plug on electric cars." http://www.bbc.com/future/story/20121120-pulling-the-plug-on-electric-cars, 2014.

[3] N. Tesla, "Experiments with alternate currents of very high frequency and their application to methods of artificiel illumination," *The Inventions, Researches and Writings of Nikola Tesla*, 1891.

[4] NOWI-energy, "Nowi: Enabling the internet of things." https://www.nowi-energy.com/, 2018.

[5] Drayson Technologies and LTD. Incorporated, "Freevolt rf energy harvesting - for the low energy internet of things." http://www.getfreevolt.com, 2018.

[6] Powercast Corp., "Powercast - wireless power products." http://www.powercastco.com/, 2018.

[7] H. Visser and R. Vullers, "Rf energy harvesting and transport for wireless sensor network applications: Principles and requirements," *Proceedings of the IEEE*, 2013.

[8] D. Snoonian, "Smart buildings," *IEEE Spectrum*, 2003.

[9] Beghelli Canada, "Iec 60529-1 & nema standards." https://www.brenclosures.com.au/wp-content/uploads/BR-Enclosures_IP-Ratings-Chart.pdf, 2003.

[10] E. E. Bronkhorst and D. L. J. Kappelle, "Autonomous battery less sensor for iot applications in smart buildings: Low-power processing & communication," tech. rep., University of Technology Delft, 2018.

[11] B. Meekes and V. J. F. R. Waegenaere, "Autonomous battery less sensor for iot applications in smart buildings: Ambient rf energy harvesting in office environment for iot sensor," tech. rep., University of Technology Delft, 2018.

[12] M. Stoopman, "Circuit design for highly sensitive rf-powered wireless sensor nodes," Master's thesis, TU Delft Bio-Electronics, 2009.

[13] S. Kitazawa, H. Ban, and K. Kobayashi, "Energy harvesting from ambient rf sources," *IEEE MTT-S International Microwave Workshop Series on Innovative Wireless Power Transmission: Technologies, Systems, and Applications*, 2012.

[14] K. Kotani and T. Ito, "High efficiency cmos rectifier circuit with self-vth-cancellation and power regulation functions for uhf rfids," *IEEE Asian Solid-State Circuits Conference*, 2007.

[15] V. Marian, C. Vollaire, B. Allard, and J. Verdier, "Low power rectenna topologies for medium range wireless energy transfer," *Power Electronics and Applications (EPE 2011)*, 2011.

[16] M. Pinuela, P.D. Mitcheson, and S. Lucyszyn, "Analysis of scalable rectenna configurations for harvesting high frequency ambient radiation," *The 10th International Workshop on Micro and Nanotechnology for Power Generation and Energy Conversion Applications*, 2010.

[17] T. Ungan and L. M. Reindl, "Harvesting low ambient rf-sources for autonomous measurement systems," *IEEE International Instrumentation and Measurement Technology Conference Victoria*, 2008.

[18] M. Piñuela, P. Mitcheson, and S. Lucyszyn, "Ambient rf energy harvesting in urban and semi-urban environments," *IEEE Transactions on microwave theory and techniques*, 2013.

[19] A.L. Rodrigues Mansano, "Radio frequency energy harvesting and low power data transmission for autonomous wireless sensor nodes," Master's thesis, TU Delft Bio-Electronics, 2016.

[20] U. Olgun, , Chi-Chih Chen, and J. Volakis, “Investigation of rectenna array configurations for enhanced rf power harvesting,” *IEEE Antennas and wireless propagation letters*, 2011.

[21] U. Muncuk, K. Alemdar, J. Sarode, and K. Chowdhury, “Multi-band ambient rf energy harvesting circuit design for enabling battery-less sensors and iots,” *IEEE Internet of Things Journal*, 2018.

[22] R. S. Elliott, *Antenna Theory & Design.* Wiley-IEEE Press, 2003.

[23] J.-P. Curty, N. Joehl, F. Krummenacher, C. Dehollain, and M. J. Declercq, “A model for μ-power rectifier analysis and design,” *IEEE Transactions on circuits and systems*, 2005.

[24] W.A. Serdijn, A.L.R. Mansano, and M. Stoopman, *Wearable Sensors Fundamentals, Implementation and Applications.* Elsevier Inc., 2015.

[25] P. Nintanavongsa, U. Muncuk, David Richard Lewis, and Kaushik Roy Chowdhury, “Design optimization and implementation for rf energy harvesting circuits,” *IEEE Journal on Emerging and Selected Topics in Circuits and Systems*, 2012.

[26] H. Jabbar, Y. Song, and Taikyeong T. Jeong, “Rf energy harvesting system and circuits for charging of mobile devices,” *IEEE Transactions on Consumer Electronics*, 2010.

[27] H. Yan, M. Montero, J. Gabriel, A. Akhnoukh, and L. C. N. De Vreede, “An integration scheme for rf power harvesting,” 2005.

[28] S. Daskalakis, A. Georgiadis, A. Bletsas, and C. Kalialakis, “Dual band rf harvesting with low-cost lossy substrate for low-power supply system,” *10th European Conference on Antennas and Propagation (EuCAP)*, 2016.

[29] Texas Instruments, “Bq25504 ultra low-power boost converter with battery management for energy harvester applications.” http://www.ti.com/lit/ds/symlink/bq25504.pdf, 2015.

[30] S. Priya and D.J. Inman, *Energy Harvesting Technologies.* Energy Harvesting Technologies, 2009.

[31] Ryo Umesao, Jiro Ida, Masanari Mabuchi, Yuta Kunori, Sou Tashino, Takayuki Mori, Hiroshi Miyagoshi, Keisuke Noguchi, and Kenji Itoh, “High efficiency rf energy harvesting with threshold-votlage-adjusted gate control diode,” *IEEE Faible Tension Faible Consommation*, 2014.